Field-induced electron transport and phonon dynamics in a GaAs-based *p*-*i*-*n* nanostructure: A subpicosecond time-resolved Raman probe

E. D. Grann and K. T. Tsen

Departments of Physics and Astronomy, Arizona State University, Tempe, Arizona 85287

D. K. Ferry

Department of Electrical Engineering, Arizona State University, Tempe, Arizona 85287

A. Salvador, A. Botcharev, and H. Morkoc

Coordinated Science Laboratory, University of Illinois, Urbana, Illinois 61801

(Received 5 August 1996; revised manuscript received 28 April 1997)

Electron transport and phonon dynamics in a GaAs-based *p*-*i*-*n* nanostructure under the application of an electric field have been studied by time-resolved Raman spectroscopy at $T = 80$ K. The time evolution of electron density, electron distribution, electron drift velocity, and LO-phonon population has been directly measured with subpicosecond time resolution. Our experimental results show that, for a photoexcited electron-hole pair density of $n \cong 10^{17}$ cm^{-3}, the effects of the drifting of electrons and electron intervalley scattering processes govern electron transport properties as well as the LO-phonon dynamics. All of the experimental results are compared with ensemble Monte Carlo simulations and satisfactory agreement is obtained. [S0163-1829(97)08539-1]

I. INTRODUCTION

The investigation of electron-transport properties has been of interest since the first development of semiconductor devices. This is because the understanding of how an electron moves in a semiconductor is indispensable for a device engineer to design an efficient semiconductor device. The study of electron transport properties is especially important as the size of the devices becomes smaller than 0.2 μm since, under such circumstances, the information obtained from the steady-state transport is no longer applicable and transient electron transport becomes dominant.[1,2]

Because of the potential for greatly enhancing the operating speed of semiconductor devices, transient electron-transport phenomena in semiconductors—especially electron velocity overshoot, which was first predicted theoretically by Ruch[3] in 1972—has attracted much attention.[4–9] Direct measurement of the electron velocity overshoot has proven difficult. Recently, Grann *et al.*[10–12] have measured electron distributions and electron drift velocities in a GaAs-based *p*-*i*-*n* nanostructure using transient subpicosecond Raman spectroscopy, and have directly confirmed the existence of this transient phenomenon in semiconductors. In this paper, we report the time evolution of photoexcited electron-hole pair density, electron distribution, electron drift velocity, and LO-phonon population in a GaAs-based *p*-*i*-*n* nanostructure semiconductor by using subpicosecond time-resolved Raman spectroscopy. The experimental results have been shown to be intimately connected to the interplay between the effect of the drifting of electrons due to the application of an electric field and the effect of electron intervalley scattering processes. The experimental results are compared with ensemble Monte Carlo simulations and the agreement is found to be quite satisfactory.

II. SAMPLE AND EXPERIMENTAL TECHNIQUE

The GaAs sample investigated in this work was a mesa-like GaAs-based *p*-*i*-*n* nanostructure semiconductor grown by molecular-beam epitaxy. The details of the sample structure and parameters have been described elsewhere.[11] The *p*- and *n*-type layers serve as two capacitor plates and provide a uniform electric field across the intrinsic layer, which is the region probed in our light-scattering experiments.

The laser used in this experiment had a photon energy of 1.951 eV and a pulse width of $\cong 600$ fs. These ultrashort pulses were generated by a double-jet DCM dye laser that was synchronously pumped by the second harmonic of a mode-locked cw Nd-YAG (yttrium aluminum garnet) laser operating at a repetition rate of 76 MHz.[13] The photoexcited electron-hole pair density was estimated from the power density per laser pulse, the laser spot size on the sample, and the penetration depth of the laser under our experimental conditions. We note that, because the band gap of the AlAs layer in the *p*-type region is greater than 1.951 eV, both the incident and the scattered light are unaffected by the presence of the *p*-type layer. In our pump-probe configuration, the laser pulses were split into two beams of equal intensity but perpendicular polarization. The zero time delay at the sample was determined to within ± 200 fs by the observance of the interference effect that occurred when the pump and the probe pulses were spatially and temporally overlapped.

The single-particle scattering (SPS) experiments were carried out in the backscattering geometry with $Z(X,X)\bar{Z}$ and $Z(X,Y)\bar{Z}$ scattering configurations for the pump and the probe pulses, respectively; where $X = (100)$, $Y = (010)$, and $Z = (001)$. Since the SPS cross section is inversely proportional to the effective mass of the carriers,[14,15] our experiment primarily probes electron transport in the Γ valley, even though holes are simultaneously present. We note that,

under reverse-biased conditions, our backscattering geometry probes the electron distribution along the direction of $-\mathbf{E}$. In order to easily observe the LO-phonon signal, a backscattering geometry was used with $Z(X',Y')\overline{Z}$ and $Z(X',X')\overline{Z}$ for the pump and the probe pulses, respectively; where $X'=(110)$ and $Y'=(1\overline{1}0)$. All of the experimental data reported here were performed at $T=80$ K. The scattered light was collected and analyzed by a double spectrometer and a photomultiplier tube (for detecting SPS signal) and a charge-coupled-device detector (for the detection of LO phonons).

In our time-resolved Raman experiments, three different Raman spectra were taken for each time delay Δt: (a') both the pump and the probe pulses are present; (b') the pump pulse only; and (c') the probe pulse only. Each of the spectra has luminescence background from both the E_0 and $E_0+\Delta$ band gaps of GaAs. First of all, as demonstrated in detail in Ref. 11, the luminescence background from both the E_0 and the $E_0+\Delta$ band gaps of GaAs is properly subtracted in each of the spectra. We refer to the corresponding subtracted Raman spectra as (a), (b), and (c), respectively. Time-resolved Raman spectra are then obtained by a computational subtraction procedure of these subtracted spectra: $(a)-[(b)+(c)]$.[16] For example, in the case of SPS scattering experiments, the resultant spectrum is interpreted as the Raman spectrum of photoexcited electrons created by the pump pulse and detected by the probe pulse delayed by Δt. In the following, all the Raman spectra shown for each time delay Δt have been so processed. Because the photoexcited electron-hole pair density is low (10^{17} cm^{-3}) in our experiments, the effects of carrier screening on the average electric-field intensity the electrons experience is minimal. In other words, the electric-field intensity inside the scattering volume is approximately given by $E=(V_{\text{app}}-V_{\text{bi}})/d$, where V_{app} is the applied voltage, V_{bi} ($=-1.5$ V at $T=80$ K) is the built-in voltage, and d ($=1$ μm) is the thickness of the intrinsic layer.

III. EXPERIMENTAL RESULTS AND ANALYSIS

Figure 1 shows a typical set of SPS spectra for a GaAs-based *p-i-n* nanostructure taken at $T=80$ K, with photoexcited electron-hole pair density of $n\cong10^{17}$ cm^{-3}, an electric-field intensity of $E=15$ kV/cm, and a time delay of $\Delta t=-330$ fs. Figures 1(a), 1(b), 1(c), and 1(d) are the pump +probe, pump only, probe only, and nonequilibrium signal ($=(a)-[(b)+(c)]$), respectively. Following detailed discussions in Ref. 12, the nonequilibrium SPS signal of Fig. 1(d) can be easily transformed into the nonequilibrium electron distribution along the direction of the wave vector transfer $\mathbf{q}\equiv\mathbf{k}_i-\mathbf{k}_s$, where $\mathbf{k}_i$ and $\mathbf{k}_s$ are the wave vectors of the incident and scattered photons, respectively.

The electron distribution thus obtained is shown in Fig. 2(a) (open circles) for an electron density of $n\cong10^{17}$ cm^{-3}. The drift velocity for a given electron distribution function was calculated in a straightforward way by taking a weighted average over the electron velocity distribution.

Two features in the electron distribution are worthwhile mentioning: First, the electron distribution is in general shifted toward the positive-velocity side of the spectrum
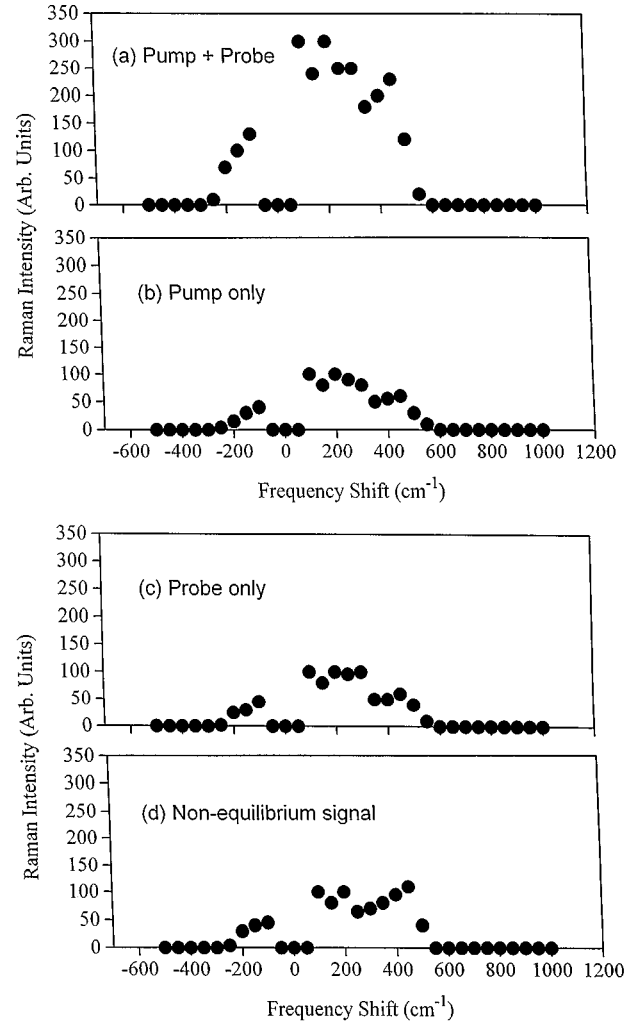

FIG. 1. A typical set of single-particle scattering spectra for a GaAs-based *p-i-n* nanostructure semiconductor, taken at $T=80$ K, with a photoexcited electron-hole density of $n\cong10^{17}$ cm^{-3}, an electric-field intensity of $E=15$ kV/cm, and at a time delay of $\Delta t=-330$ fs. (a), (b), and (c) refer to pump and probe pulses both present, pump pulses only, and probe pulses only, respectively. (d) is obtained from (a)$-$[(b)+(c)], and represents nonequilibrium Raman signal excited from the pump pulses and detected by the probe pulses.

(which is the direction of $-\mathbf{E}$), as expected. Furthermore, it is neither a Maxwell-Boltzman nor a Fermi-Dirac function. Second, the electron distribution falls off very rapidly at around 1.1×10^8 cm/sec, which indicates the onset of electron intervalley scattering processes in GaAs.

Figure 2 shows electron distributions (open circles) at various time delays ranging from $\Delta t=-330$–1320 fs and for an electric-field intensity of $E=15$ kV/cm. For the sake of clarity, the scale of electron distributions has been properly normalized so that they are readily compared. A summary of the electron density, the electron drift velocity as a function of the time delay, is shown in Figs. 3 and 4 (open circles). We note that the shape of electron distribution is different for various time delays. In addition, the electron density, which is proportional to the integrated area under the electron distribution, is found to first increase slightly and then decrease at the long-time delays. We interpret these
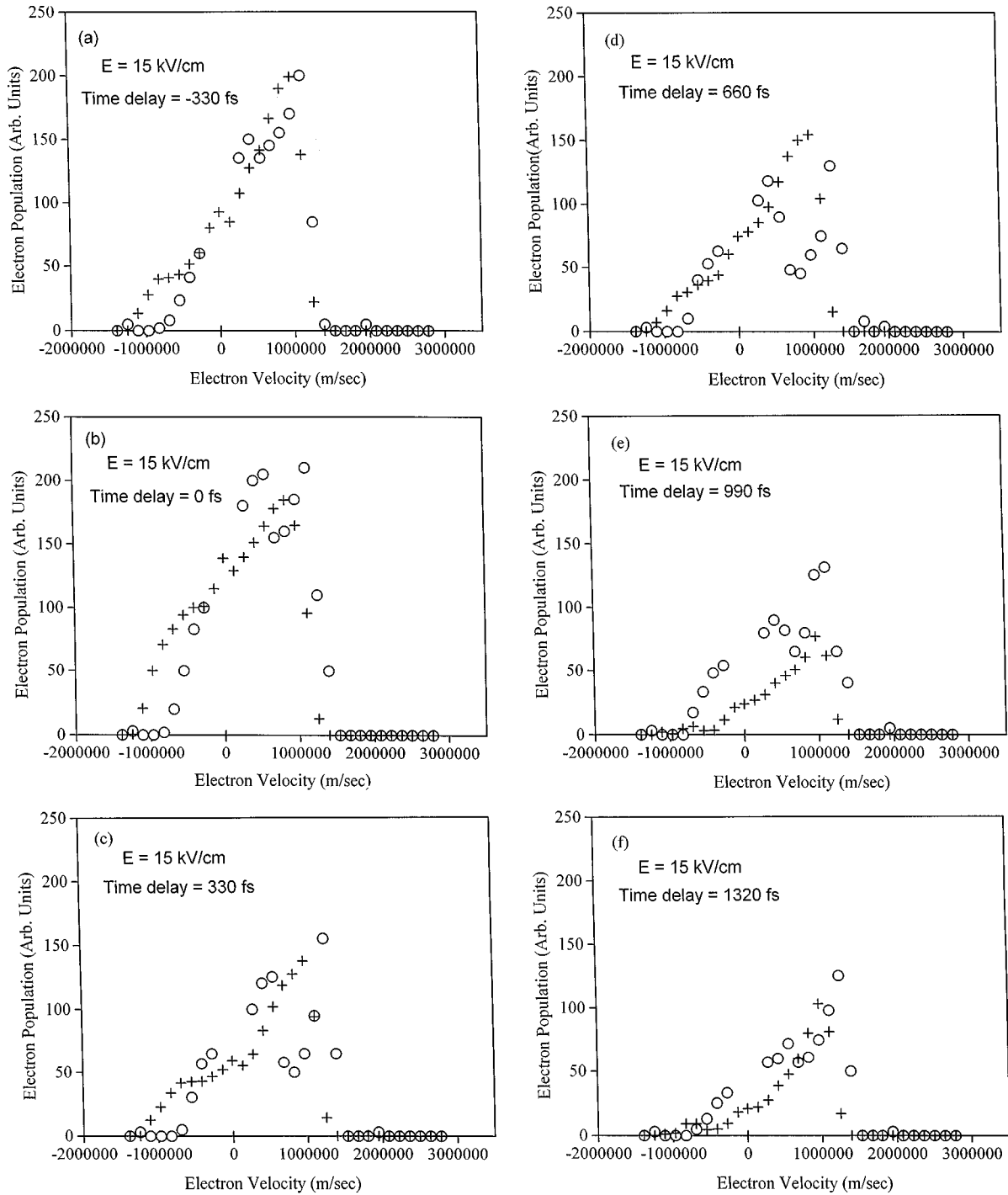
FIG. 2. Measured nonequilibrium electron distributions in a GaAs-based p-i-n nanostructure (open circles) are compared with EMC simulations (crosses), for the time delay $\Delta t =$ (a) -330 fs; (b) 0 fs; (c) 330 fs; (d) 660 fs; (e) 990 fs, and (f) 1320 fs, and for an electric-field intensity of $E = 15$ kV/cm.

experimental results as the interplay of two effects: the drifting of electrons as a result of the application of an electric field and electron intervalley scattering processes. The effect of the drifting of electrons tends to reduce the electron density and to increase the electron drift velocity probed in our light-scattering experiments; whereas the effect of electron intervalley scattering processes increases (decreases) the electron density for satellite to central valleys (central to satellite valleys) scattering processes, and reduces the electron drift velocity. The initial increase of electron density from the time delay $\Delta t = -330$ to 0 fs is due primarily to the overlapping of the pump and the probe pulses. The relatively sharp decrease between 0 and 330 fs is because of the effect of the drifting of electrons as well as the effect of central to satellite intervalley scattering processes. As the time delay increases further, the electron density decreases even more, suggesting that the number of electrons drifting away from the probed region is larger than that scattered back from the satellite valleys to the central valley. We note that if the effect of the drifting of electrons is the only factor influenc-
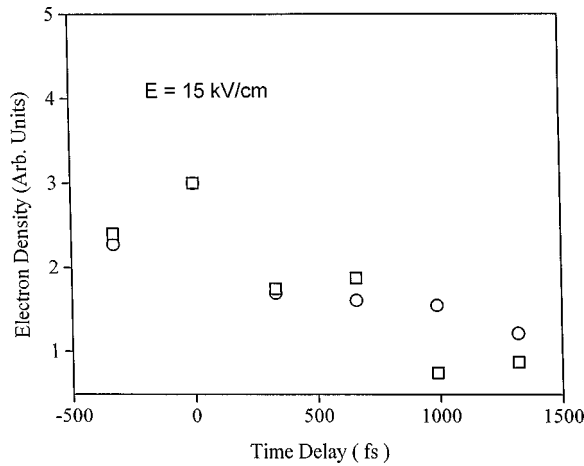
FIG. 3. Experimentally deduced electron densities (open circles) as a function of time delay in a GaAs-based *p-i-n* nanostructure semiconductor are compared with EMC simulations (open squares) for an electric-field intensity of $E = 15$ kV/cm.

ing electron transport in our experiments, then one would not expect to observe electrons with relatively large negative electron velocities in the electron distributions at the long-time delays such as $\Delta t = 660$, 990, and 1320 fs. This is obviously in contradiction with the experimental data of Fig. 2. Therefore, we believe that the effect of intervalley scattering processes also plays an important role in the determination of electron distributions. The Jones-Rees effect[17] is a result of the fact that the electrons suffering intervalley scattering tend to have their final wave vectors opposite to the direction of the acceleration by the applied electric field. The presence of relatively large negative electron velocities at the long-time delays observed in our experiments is consistent with such an effect. The slight increase of the electron drift velocity as the time delay increases suggests that the effect of the drifting of electrons is more important than that of electron intervalley scattering processes, in particular, at the long-time delays.

Figure 5 shows the nonequilibrium LO-phonon population (solid circles) as a function of the time delay for a GaAs-
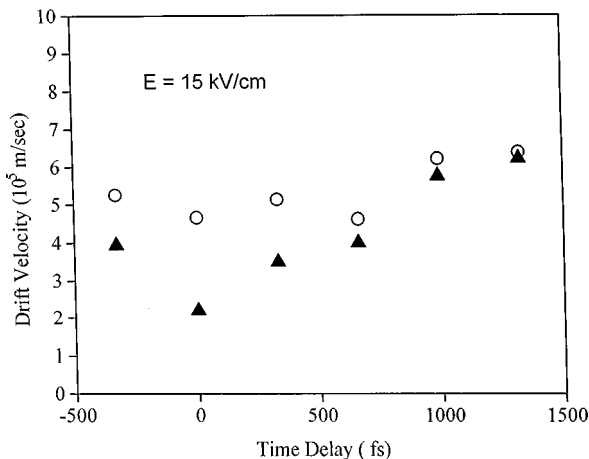

FIG. 4. Experimentally deduced electron drift velocities (open circles) as a function of time delay in a GaAs-based *p-i-n* nanostructure semiconductor are compared with EMC simulations (solid triangles) for an electric-field intensity of $E = 15$ kV/cm.
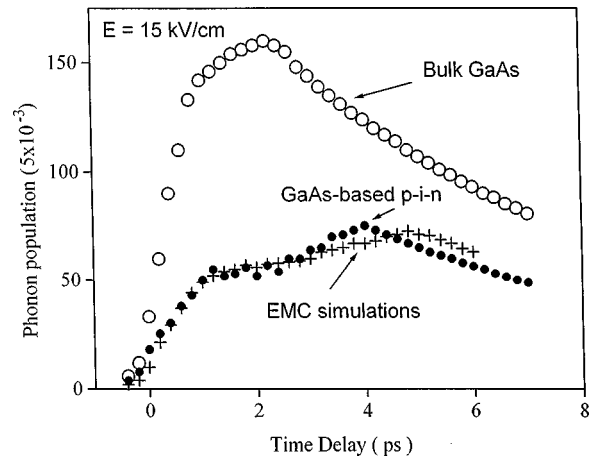

FIG. 5. Measured nonequilibrium LO-phonon populations as a function of time delay for a GaAs-based *p-i-n* nanostructure semiconductor (solid circles) are compared with EMC simulations (crosses) for an electric-field intensity of $E = 15$ kV/cm. The results for a bulk GaAs sample (open circles) are also shown for comparison.

based *p-i-n* nanostructure semiconductor taken at $T = 80$ K, with a photoexcited electron-hole pair density of $n \cong 10^{17}$ cm^{-3}, for an electric-field intensity of $E = 15$ kV/cm. For comparison, the result of a bulk GaAs sample taken under exactly the same experimental conditions, except for $E = 0$ (open circles), is also shown. We have found that, not only is the nonequilibrium LO-phonon population much smaller in the GaAs-based *p-i-n* nanostructure than in the bulk GaAs, but also the peak of the population is shifted toward longer time delay (from $\cong 2$ ps for the bulk GaAs to $\cong 4$ ps for the GaAs-based *p-i-n* nanostructure). We explain these experimental results again in terms of the effect of the drifting of electrons and that of the electron intervalley scattering processes as follows: First of all, the observed peak nonequilibrium LO-phonon population is significantly smaller in the GaAs-based *p-i-n* nanostructure than in bulk GaAs. This is primarily due to the drifting of electrons away from the probed region as a result of the application of an electric field. We note that, since the group velocity of the LO phonons is almost zero, once the energetic electrons leave the probed region, the LO phonons they emit cannot be detected in our Raman experiments. Second, because it takes approximately 2–3 ps (as extrapolated from Fig. 2) for the electrons to leave the probed region, and it also takes about 2 ps for these energetic electrons to emit all the Raman-active LO phonons,[18] we expect that the maximum of the observed nonequilibrium LO-phonon population in the GaAs-based *p-i-n* nanostructure should occur at around 4–5 ps. This prediction is in very good agreement with what has been observed in Fig. 5

IV. ENSEMBLE MONTE CARLO SIMULATIONS

We have performed ensemble Monte Carlo (EMC) simulations under our experimental conditions in order to get better insight into the electron transport and phonon dynamics in the GaAs-based *p-i-n* nanostructure. Simulations of the laser-excited plasma were carried out with an ensemble Monte Carlo technique.[19] In the simulation, only the elec-

trons were considered, as the population of the polar LO-phonon modes was of primary interest. Hyperbolic energy bands were assumed for the various conduction bands, and all normal scattering processes were included. Modeling of the nonequilibrium phonons was handled within the EMC procedure by a secondary self-scattering and rejection process pioneered by Lugli et al.[20] The buildup of the phonon population through the emission and absorption processes was monitored throughout the simulation. The difference between the instantaneous value, for a given momentum wave vector, and some prescribed maximum value was used for the rejection technique.[21] The presence of these nonequilibrium phonons slows the decay of the hot carriers.

The carrier-carrier interaction is very important at high carrier densities. Each carrier, while interacting with the phonons, is also affected by the other carriers, which effectively screens the electron-phonon interaction. Because of the long simulation time and large number of particles used (30 000), our normal real-space molecular-dynamics approach to the carrier-carrier scattering was not used. Rather, an approach described by Osman and Ferry[22] was adopted, in which a dynamically screened carrier-carrier scattering process in momentum space is added to the simulation. Here, the carriers are scattered only by those electrons within the same conduction-band valley, and in the same region of the p-i-n structure. The screening wave vector is continuously reevaluated during the simulation, and the strength of the carrier-carrier scattering adjusted to account for the temporal variation of both the number of carriers, and their distribution function, in the i region of the structure.

Particles are assumed to be generated in the intrinsic region of the GaAs-based p-i-n structure, with a positional probability determined by the attenuation of absorption into the material from the laser-illuminated front surface. These particles are then allowed to evolve, and cool, under the influence of the electric field. Special treatment is accorded to the particles as they reach the heterojunction interfaces at the ends of the central portion (i region) of the structure. Particles with sufficient energy to surmount the heterostructure band discontinuity are allowed to move into the AlAs layers, and are removed from the simulation that generates the Raman signal and the nonequilibrium phonon distribution. Those with insufficient energy to surmount the barrier are assumed to undergo diffusive interface scattering, thus being reflected back into the central region. The Raman signal is then estimated by computing the population of both electrons and phonons, and weighting them by the absorption undergone in photon transmission through the active i region.

As can be seen from the set of data in Figs. 2–4, the computed electron distribution functions agree quite well with those determined experimentally. The peak of the distribution is generally found to be at a velocity of about 1×10^8 cm/sec, which is actually limited by the band-structure details assumed in the hyperbolic model, although the energy distribution is relatively uniform up to the thresh-old for intervalley scattering. This value agrees with a number of pseudopotential calculations, but the uncertainty of this value from various assumptions in the theory is at least 20%. For this reason, we have not adjusted the hyperbolic model to fit the slightly higher value suggested in the experimental data of Figs. 2–4.

V. DISCUSSIONS

The results of EMC simulations (crosses) are compared with the experimental data for electron distributions at various time delays as specified in Fig. 2. Qualitatively, the fit is quite satisfactory except in the regions around -1×10^8 and 1.2×10^8 cm/sec. As discussed in detail in Refs. 11 and 12, these discrepancies are most likely due to the specific details of the hyperbolic band assumed in the EMC simulations as well as the manner in which electron scattering at the p-type interface is handled in the EMC simulations.

We note that the deviations between the experimental results and the EMC simulations are greater for the longer-time delays. We believe that this is primarily due to the greater errors as a result of the manipulations of relatively smaller signal at the longer-time delays.

In comparison of the nonequilibrium LO-phonon population (Fig. 5), we find that EMC calculations are in good agreement with the experimental results. They both give a peak LO-phonon population of about 70 times larger than that in the equilibrium lattice at $T = 80$ K. We note that the peak position occurs at 4.0 ps in the experimental data; whereas, at 4.8 ps in the EMC simulations. However, since the LO-phonon population is quite ''flat'' in this time range, the difference is not considered significant.

VI. CONCLUSIONS

We have studied transient electron transport as well as LO-phonon dynamics in a GaAs-based p-i-n nanostructure semiconductor under the application of high electric fields by using subpicosecond time-resolved Raman spectroscopy. The time evolution of electron distribution, electron density, electron drift velocity, and LO-phonon populations was directly measured with subpicosecond time resolution. These experimental results were interpreted as the interplay of two effects: the drifting of electrons as a result of the application of an electric field, and electron intervalley scattering processes. We have also carried out ensemble Monte Carlo simulations under our experimental conditions. The comparison between our experimental results and the EMC calculations was quite satisfactory.

[1] D.K. Ferry, H.L. Grubin, and G.J. Iafrate, in *Semiconductors Probed by Ultrafast Laser Spectroscopy*, edited by R.R. Alfano (Academic, New York, 1984), Vol. 1, p. 413.

[2] E. Constant, in *Hot Electron Transport in Semiconductors*, edited by L. Reggiani (Springer, Berlin, 1985), p. 227.

[3] J.G. Ruch, IEEE Trans. Electron Devices **ED-19**, 652 (1972).

[4] T.J. Maloney and J. Frey, J. Appl. Phys. **48**, 781 (1977).

[5] M.S. Shur and L.H. Eastman, Solid-State Electron. **24**, 11 (1981).

[6] C.V. Shank, R.L. Fork, B.I. Greene, F.K. Reinhart, and R.A. Logan, Appl. Phys. Lett. **38**, 104 (1981).

[7] K.E. Meyer, M. Pessot, G. Mourou, R.O. Grondin, and S.N. Chaoun, Appl. Phys. Lett. **53**, 2254 (1988).

[8] J. Son, W. Sha, J. Kim, T.B. Norris, J.F. Whitaker, and G.A. Mourou, Appl. Phys. Lett. **63**, 923 (1993).

[9] E.D. Grann, S.J. Sheih, C. Chia, K.T. Tsen, O.F. Sankey, S.E. Guncer, D.K. Ferry, G. Maracas, R. Droopad, A. Salvador, A. Botcharev, and H. Morkoc, Appl. Phys. Lett. **64**, 1230 (1994).

[10] E.D. Grann, K.T. Tsen, O.F. Sankey, D.K. Ferry, A. Salvador, A. Botcharev, and H. Morkoc, Appl. Phys. Lett. **67**, 1760 (1995).

[11] E.D. Grann, S.J. Sheih, K.T. Tsen, O.F. Sankey, S.E. Guncer, D.K. Ferry, A. Salvador, A. Botcharev, and H. Morkoc, Phys. Rev. B **51**, 1631 (1995).

[12] E.D. Grann, K.T. Tsen, D.K. Ferry, A. Salvador, A. Botcharev, and H. Morkoc, Phys. Rev. B **53**, 9838 (1996).

[13] K.T. Tsen and H. Morkoc, Phys. Rev. B **38**, 5615 (1988).

[14] M. V. Klein, in *Light Scattering in Solids I*, edited by M. Cardona and G. Guntherodt (Springer, Berlin, 1983), p. 147.

[15] G. Abstreiter, M. Cardona, and A. Pinczuk, in *Light Scattering in Solids IV*, edited by M. Cardona and G. Guntherodt (Springer, Berlin, 1983), p. 5.

[16] K. Tanaka, H. Ohtake, and T. Suemoto, Phys. Rev. Lett. **71**, 1935 (1993).

[17] D. Jones and H.D. Rees, Electron. Lett. **8**, 363 (1972); see also D.K. Ferry and R.O. Grondin, *Physics of Submicron Devices* (Plenum, New York, 1991), pp. 198–201.

[18] J.A. Kash, J.C. Tsang, and J. M. Hvan, Phys. Rev. Lett. **54**, 2151 (1985).

[19] D.K. Ferry, A.M. Kriman, M.-J. Kann, and R.P. Joshi, in *Monte Carlo Device Simulation: Full Band and Beyond*, edited by K. Hess (Kluwer, Norwall, MA, 1991), p. 99.

[20] P. Lugli, C. Jacoboni, L. Reggiani, and P. Kocevar, Appl. Phys. Lett. **50**, 1251 (1987).

[21] D.K. Ferry, *Semiconductors* (Macmillan, New York, 1991).

[22] M.A. Osman and D.K. Ferry, Phys. Rev. B **36**, 6018 (1987).